CELL CYCLE
2020, VOL. 19, NO. 14, 1786–1803
https://doi.org/10.1080/15384101.2020.1780381

Taylor & Francis
Taylor & Francis Group

RESEARCH PAPER

Cyclin E and Cdk1 regulate the termination of germline transit-amplification process in *Drosophila* testis

Purna Gadre, Shambhabi Chatterjee, Bhavna Varshney, and Krishanu Ray

Department of Biological Sciences, Tata Institute of Fundamental Research, Mumbai, India

ABSTRACT

An extension of the G1 is correlated with stem cell differentiation. The role of cell cycle regulation during the subsequent transit amplification (TA) divisions is, however, unclear. Here, we report for the first time that in the *Drosophila* male germline lineage, the transit amplification divisions accelerate after the second TA division. The cell cycle phases, marked by Cyclin E and Cyclin B, are progressively altered during the TA. Antagonistic functions of the *bag-of-marbles* and the Transforming-Growth-Factor-β signaling regulate the cell division rates after the second TA division and the extent of the Cyclin E phase during the fourth TA division. Furthermore, loss of Cyclin E during the fourth TA cycle retards the cell division and induces premature meiosis in some cases. A similar reduction of Cdk1 activity during this stage arrests the penultimate division and subsequent differentiation, whereas enhancement of the Cdk1 activity prolongs the TA by one extra round. Altogether, the results suggest that modification of the cell cycle structure and the rates of cell division after the second TA division determine the extent of amplification. Also, the regulation of the Cyclin E and CDK1 functions during the penultimate TA division determines the induction of meiosis and subsequent differentiation.

ARTICLE HISTORY
Received 28 November 2019
Revised 1 May 2020
Accepted 4 June 2020

KEYWORDS
Cyclin E; CDK1; germline stem cells; transit-amplification; testis; *drosophila*

Introduction

A balance between proliferation and differentiation is critical during development for tissue growth and patterning, and in adults for maintaining tissue homeostasis. The transit amplification (TA) divisions of the stem cell progeny generate a pool of progenitor cells that can act as a buffer limiting the proliferative stress on the stem cells during tissue regeneration [reviewed in 1, 2, 3], which helps to maintain the stem cells for a longer duration during the lifetime of an organism. The proliferative pool of tissue progenitors undergoes a change from a stem-cell-like to a differentiated-cell-like identity. Typically, an extension of the G1 phase is considered to induce differentiation [*reviewed in* 4], and induction of differentiation often leads to expression of inhibitors of G1-S transition [5, 6, *reviewed in* 7]. Previous studies suggested that a molecular clock intrinsic to the proliferative progenitor cells controls the timing of differentiation [8], and the number of TA divisions within this time-scale is determined according to the cell cycle lengths of the progenitor cells [9,10]. Hence, understanding the role of cell cycle regulation during the TA is necessary to unravel the interplay between the rates of cell divisions and differentiation.

The *Drosophila* germline is a well-suited model system for assessing the correlation between cell cycle regulation and differentiation during the TA divisions. The asymmetric division of a germline stem cell (GSC) produces the progenitor, gonialblast (GB), which undergoes four rounds of symmetric TA divisions, forming 2, 4, 8, and 16 interconnected gonial cells. Subsequently, either one (in the ovary) or all (in testis) of the 16 gonial cells enter meiosis [11, Reviewed in 12]. GSCs and early gonial cells in testis express an RNA binding protein, Held-out-wing (How), which suppresses the differentiation program [13]. The gonial cells in testis at the 4- and 8-cell stages express the *bag-of-marble* (*bam*) gene [10]. The presence of Bam protein stabilizes Cyclin A [14], suppresses the expression of stem cell maintenance factors [15,16], and promotes differentiation of the gonial cells in the ovary. Bam accumulates to a critical level at the 8-cell stage, which is suggested to arrest

CONTACT Krishanu Ray krishanu@tifr.res.in

the TA after one extra round, and loss of Bam protein through a translational regulation triggers the onset of meiosis at the 16-cell stage [10]. Ectopic Bam overexpression, however, does not induce premature differentiation before the 8-cell stage [10,17]. Thus, Bam appeared to act as a modulator of the developmental clock. The secretion of Bone Morphogenetic Proteins (BMP), decapentaplegic (dpp), and glass-bottom-boat (gbb), form the somatic niche [18], and cell-autonomous regulation [19] represses the *bam* expression in GSCs and GBs in testis. Hence, the length of the second TA division must be adjusted to coincide with the Bam expression at the 4-cell stage.

After TA, the germline cells in the ovary and testis adopt distinct cell fates. In the ovary, only one of the 16 oogonial cyst cells goes through meiosis, producing a single oocyte, and the rest undergoes multiple endoreplications generating 15 nurse cells. In the testis, all 16 spermatogonial cells undergo meiosis and subsequent differentiation to generate a clone of 64 spermatids. Studies in the ovary suggest that the GSCs and early gonial cells have a distinctly different cell cycle structure as compared to the later TA stages [20]. The cell cycle regulators, Cyclin E [21], Cyclin B [22], and the turnover of Cyclin A [23] are essential for the GSC proliferation and maintenance. Cyclin E, which is known to regulate the G1 length in somatic cells, expresses in an atypical manner in the female GSCs [24], and it is indicated to control both the GSC division and maintain the cell fate [21] . Further, the Cdc25/String, which is known to activate CDK1, was shown to maintain the GSC fate in the testis [25]. However, it is still unclear how the regulation of cell cycle phases during the subsequent TA process influences the germline amplification and differentiation.

In this study, we investigated the cell division rates and the pattern of cell cycle phases during the TA in *Drosophila* testis to understand their role in TA regulation. It revealed a progressive restructuring of the cell cycle with midstream acceleration during the amplification process. The genetic analysis suggested that the Bam function, antagonized by the Transforming Growth Factor β (TGFβ) signaling, regulates separate aspects of the cell cycle during the third and fourth amplificaiton divisions. The results also suggested that regulation of the G2 phase and the rates of GSC and GB divisions set the pace of the differentiation program in the male germline lineage, and regulation of the CycE and CDK1 activities during the penultimate TA division is critical for the induction of meiosis. A detailed description of our observation and analysis is provided below.

Materials and methods

Drosophila stocks and culture condition

All stocks and crosses were maintained on standard *Drosophila* medium at 25°C unless mentioned otherwise. The flies were reared for four days at 29°C before dissection and fixing, as described before [26]. The list of fly stocks is presented in Table S2.

Whole-mount immunofluorescence-staining

Testes from a four-day-old male were dissected in Phosphate buffer-saline (PBS) and fixed in 4% paraformaldehyde for 20 to 30 minutes at room temperature. The testes were then washed 3 times in PTX (0.3% Triton-X100 in PBS), incubated in blocking solution PBTX (5% BSA in and incubated with an appropriate dilution of primary antibodies overnight. Samples were washed 3 times in PTX followed by a 2-hour incubation at room temperature with Alexa dye-conjugated secondary antibodies Invitrogen) at 1:200 dilution in PBTX, and a final set of wash in PTX. The samples were mounted with a drop of Vectashield® (Vector Laboratory Inc., USA). For visualizing the nucleus, the samples were incubated with 0.001% Hoechst-33,342 (Sigma Chemical Co. USA) for 20 minutes post the entire immunostaining protocol. Then the samples were washed with PTX and mounted as mentioned above. The following primary antibodies were used: rat anti-Vasa (1:50; Developmental Studies Hybridoma Bank (DSHB); developed by A. Spradling, Carnegie Institution for Science, USA), mouse anti-Armadillo (1:100; DSHB; E. Wieschaus, Princeton University, USA), rabbit anti- phospho-Histone-3 (1:4000, Santa Cruz Biotechnology); mouse anti-cyclin A (DSHB, C.F. Lehner,

University of Bayreuth, Germany), rabbit cyclin-E (1:100, Santa Cruz Biotechnology).

Quantification of germline cell death (GCD)

For the detection of GCD, testes were stained with Lysotracker RedDND-99 (Life Technologies) in PBS for 30 min before paraformaldehyde fixation.

Image acquisition, analysis, and SG profile quantification

Images were acquired using Olympus FV1000SPD laser scanning confocal microscope using 10X, 0.3 NA and 60X, 1.35 NA, or Olympus FV3000SPD laser scanning confocal microscope using 60X, 1.42 NA objectives or Zeiss 510meta laser scanning confocal microscope using the 63X, 1.4 NA objective. Live imaging was performed using an FV3000SPD laser scanning confocal microscope at 10 × 0.40 NA or Nikon TI-E microscope at 20 × 0.75 NA Multiple optical slices were collected covering the entire apical part of the testes. The images were analyzed using ImageJ® []. The Cell-counter™ plugin was used for the quantification of the immunostained SGs. For estimating the SGs stained with different cell cycle phase markers, the images were thresholded at the 95 percentile according to the intensity histogram, and the SGs marked above the threshold were counted as positive.

Heat shock protocol

Heat shock protocol, previously described in 17, was used to overexpress bam in *hs-bam* background. 4-day old male flies, raised at 18°C, were collected in glass vials and submerged in a water bath maintained at 37°C for 30 minutes at approximately 10 AM and 6 PM. The vials were maintained at 29°C between heat shocks and were transferred to 18°C after 6PM. Testes were dissected after 24 hours.

Statistical analysis

The Origin (OriginLab, Northampton, MA) software, Graphpad online software, and Microsoft Excel (2013) was used for all statistical analysis.

Results

The spermatogonial cells divide at a relatively faster rate after the second TA division

In wild-type testes, the GSCs are arranged in a radial manner around the stem cell niche, termed as the hub (Figure 1(A,B)). The GB and the spermatogonial cells derived from a GB divide synchronously within an encapsulation formed by two somatic-origin cyst cells [27]. Together this assembly is called a cyst. The number of spermatogonial (SG) cells within the somatic enclosure defines the TA stage of the cyst (Figure 1(C)). Estimation of different TA stages in the wild-type (Canton-S) and various other genetic backgrounds, commonly used as wild-type controls, indicated a significant drop (approximately by 50%) in the population of cysts after the 2-cell stage (Figure 1(D)) [28,29]. The drop in cyst population at 4-cell stage could occur due to an acceleration of rates of divisions from the 4-cell stage onwards, or due to excessive cell death at the 2-cell or 4-cell stage. Several studies have reported that germline cells occasionally die through a non-apoptotic process, called the germ cell death (GCD) [30–32]. We observed GCD at every TA stage in the wild-type background; however, there was no sharp increase in the frequency of GCD at the 2-cell or 4-cell stages (Figure S1). Therefore, we inferred that the cell cycle rates speed-up by nearly 50% after the second TA division causing the commensurate reduction in the pool of cysts at the 4-cell stage.

Cell cycle phases are progressively remodeled during the TA divisions

Gap phase regulation is one of the significant determinants of the cell cycle length. To identify the cell cycle phases during the TA, we examined the CycE, CycA, and phospho-Histone-3 (pH3) immunostaining, and the expressions of ΔPCNA::GFP and CycB::GFP protein trap during the TA stages in the wild-type testis. The CycE staining marked occasional spermatogonial cysts, whereas the endogenous CycB::GFP expression marked all cysts at all stages with variable intensity (Figure 1(A-E)). In both these cases, we found

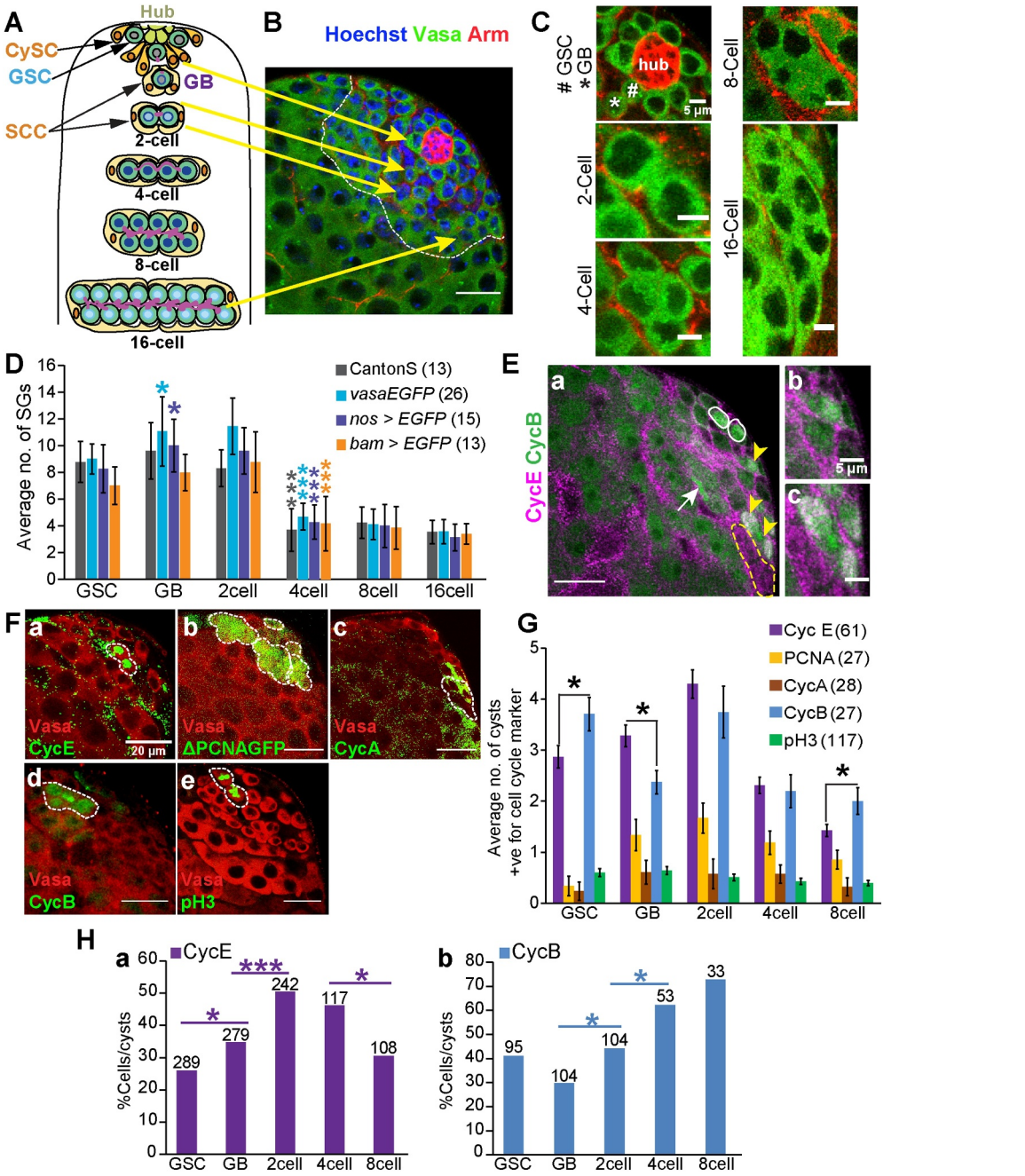

Figure 1. Analysis of the cell cycle structure during the TA divisions in the *Drosophila* testis. A) Schematic illustrates the process of transit amplification during early spermatogenesis. Glossary: GSC – Germline Stem Cell, CySC – Cyst Stem cell, SCC – Somatic Cyst Cell, GB – Gonialblast, SG – Spermatogonia. B) The apical tip of wild-type (WT) testis stained with the Hoechst-dye (blue), anti-Armadillo (Red), and anti-Vasa (green). GSC, GB, 2-cell, and 16-cell spermatogonial cysts are indicated by yellow arrows. (Scale bars ~20 µm). C) Enlarged images of the hub, GSCs, and spermatogonial cysts at different stages of TA in wild-type testis. (Scale bars ~5 µm). D) Stage-wise distribution of spermatogonial cysts (average ± S.D.) in CantonS, *vasaEGFP, nos>EGFP, bam>EGFP* backgrounds (gray bars). The pair-wise significance of difference was estimated using the Mann-Whitney-U test (p-values are * <0.05, **<0.01, ***<0.001). **E).** A GFP::CycB-expressing adult testis stained with anti-CycE. Yellow arrowheads mark the germ cells positive for both the nuclear CycE and CycB, white arrow marks fusome-like localization of CycB, white solid lines mark GSCs expressing only CycB, and broken lines mark an 8-cell cyst positive for CycE only. Enlarged images (b, c) of germ cells positive for both nuclear CycE and CycB are shown in the side panels. **F)** The apical tip of testes stained with vasa (Red) and different cell cycle markers (Green) indicates the distribution of cell cycle phases in the spermatogonial cysts at different stages. The images are generated after 95% thresholding, which revealed the distribution of peak levels of CycE (a), CycA (c), and pH3 (e) ΔPCNA-GFP (b) and GFP-CycB (d). (scale bars ~20 µm). **G)** Histograms indicate the average (± SEM) spermatogonial cysts stained with different cell cycle phase markers at each stage of the TA. The pair-wise significance of difference was estimated using the Mann-Whitney-U test (p-values are * <0.05, **<0.01, ***<0.001). **H)** Histograms indicate the fraction of spermatogonial cysts marked with the peak CycE (a), and CycB (b) staining at each stage. The pair-wise significance of difference was estimated using Fisher's exact test (p-values are * <0.05, **<0.01, ***<0.001).

occasional cysts at each stage marked with high levels of CycB::GFP (Figure 1(A-E), white circles) and CycE staining (Figure 1(A-E), yellow dotted border) in the germ cell nucleus. The CycE staining oscillated between the nucleus and cytoplasm. The CycB::GFP alternated between the cytoplasm, nucleus, and fusome-like structures (white arrow, Figure 1(E)).

To estimate the stage-specific distribution of the peak expression of CycE, ΔPCNA::GFP, CycA, and CycB::GFP during the TA, we considered the cysts that were marked above a threshold of 95-percent of the intensity levels in each image (figure 1(F)). We identified a few cysts expressing peak levels of CycB and CycE at each TA stage in every testis, comparatively fewer cysts marked by the ΔPCNA::GFP expression, and very few cysts marked by the CycA and pH3 immunostaining, respectively (Figure 1(G)). Unlike the GSCs in *Drosophila* ovary, where CycE expression overlapped with that of CycB [21], we found only limited overlap between the peak CycE staining and CycB-GFP localization in the germ cell nuclei during the GSC and TA stages (Table S1). Together, these results indicated that the CycE and CycB levels peak at separate intervals, potentially marking the G1-S and G2-M phases, respectively, during the germline cell cycle in *Drosophila* testis.

The GSCs in both the ovary and testis have a short G1 and longer G2 phases [24,33]. In the ovary, the first two divisions of the gonial cells follow a similar pattern, and the following TA divisions go through a relatively longer S and M phases [20]. We found that the average number of CycE-positive GSCs was significantly less than those marked by CycB in the testis. The distribution was reversed in the GBs (Figure 1(G)). The average numbers of CycE and CycB-positive cysts are comparable at the 2- and 4-cell stages. At the subsequent 8-cell stage, the number of CycE-positive GBs was significantly more than that of CycB (Figure 1(G)). We also noted that, though the average number of GSCs and GBs are comparable (Figure 1(D)), the number of GBs marked by the ΔPCNA::GFP was several folds higher (Figure 1(G)). These observations may suggest that the GSCs go through a comparatively shorter S-phase than the subsequent TA stages.

Next, we calculated the percentage of CycE and CycB-positive spermatogonial cysts at each stage (Figure 1(H)). The results indicated that the cell cycle phase marked by CycE increases steadily from the GSCs until the 2-cell stage, then declines (Figure 1(A-H)). We also noted a steady increase in the phase marked by CycB with each TA division (Figure 1(B-H)). Together these data indicated that the cell cycle structure of GBs is significantly different from that of the GSC, which is then gradually altered in subsequent stages, and then reverted to a GSC-like form during the penultimate TA divisions at the 8-cell stage. The mitotic indices of GSC, GB, and 2-cell stages were comparable, whereas the mitotic index of the 4-cell stage was significantly higher (Table 1), indicating that the spermatogonial divisions indeed speed up mid-TA. The remodeling of cell cycle structure was not apparently correlated to the acceleration of the cell division rates at the 4-cell stage. Therefore, we conjectured that the GBs and spermatogonia at the 2-cells stage might go through a relatively longer quiescence (G0) phase than the later stages. Alternatively, the cell cycle phases could be proportionately adjusted with the acceleration of the cell division at the 4-cell stage.

The fly-FUCCI [34] constructs under a ubiquitin promoter (Figure S2A) did not express in the male germline cells during the TA

Table 1. Mitotic index of the TA stages in the mutant and control backgrounds.

	Mitotic index (%)				
Genotype	GSC	GB	2-cell	4-cell	8-cell
nos>EGFP	7% (12/175)	7% (13/184)	7% (15/224)	15%[a] (14/96) p = 0.033	10% (19/98)
nos>tkv^{CA}	9% (11/122)	16%[b] (17/108) p = 0.027	5% (8/167)	3%[b] (4/135) p = 0.002	19% (12/62)
CantonS	7% (11/166)	7% (10/140)	6% (9/148)	16%[a] (10/62) p = 0.032	9% (4/47)
bam$^{\Delta 86}$/+	7% (5/70)	8% (5/63)	4% (3/82)	4%[b] (2/57) p = 0.031	7% (2/28)

NB:-.The mitotic index is calculated as the total number of pH3-positive cysts over the total number of Vasa-positive cysts in each category, as shown in the parenthesis.

a. The 4-cell stage was compared with the 2-cell stage of the same genetic background.

b. Compared with the value of the same TA stage in control.

The significance values were calculated using Fisher's Exact test.

(spermatogonial) stages (Figure S2B). However, spermatocytes expressed both GFP::E2F and RFP::CycB (Figure S2B). Hence, it was not possible to independently estimate the relative durations of the cell cycle phases using the fly-FUCCI reagent.

The upregulation of BMP signaling and partial loss of *bam* alters the rate of TA divisions.

In *Drosophila* testis, the expression of the differentiation factor, Bam, which commences at the 4-cell stage [10], coincides with the apparent acceleration of cell divison. A gradient of BMP emanating from the hub and somatic cyst stem cells (CySCs) activates the TGFβ signaling and represses *bam* expression in the GSCs and GBs, maintaining the stem cell-like nature of these cells [18,35]. Bam stabilizes cyclin A and promotes GSC differentiation in the female germline [14]). However, the role of Bam in the cell cycle regulation in male germline remains unknown. Therefore, to test the role of Bam in cell cycle regulation during the TA, we expressed a constitutively active form of the BMP receptor, thickveins (*UAS-tkv*^{CA}), and the ligand, dpp (*UAS-dpp*), using *nosGal4vp16*. We enumerated the distribution of total, as well as the CycE and pH3-positive cysts in these testes. A similar experiment was performed in the heterozygous *bam* mutant background (*bam*$^{\Delta 86}$/+).

Consistent with the previous report, we observed an accumulation of over proliferating cysts containing more than 16 spermatogonia in the *nos>tkv*^{CA} (Figure S3) and *nos>dpp* backgrounds (Figure S4). Also, there was a significant increase in the number of GSCs, 2-cell, and 4-cell cysts in *nos>tkv*^{CA} (Figure 2(B-A)) and that of the GSC population in the *nos>dpp* backgrounds (Figure S4). Due to high density, we were unable to quantify the cyst distribution in the *nos>dpp* testes. The increase in the GSC population is attributed to the role of BMP signaling in germline stem cell maintenance [18]. We also noted that the increased BMP/TGFβ signaling could delay the apparent shortening of the cell cycle length after the second TA division. In the wild-type testis, the average numbers of 4- and 8-cell cysts are nearly 50% less than the 2-cell cysts. In the *nos>tkv*^{CA} background, the average number of 4-cell cysts was comparable to that of the 2-cell population, and that of the 8-cell cysts was significantly reduced by approximately 50% (Figure 2(B-A)), suggesting that the elevation of the type-1 TGFβ signaling may prolong the third amplification division, or accelerate the first two divisions. The upregulation of TGFβ signaling is unlikely to revert the spermatogonia to the GCS-like fate because the fusome morphology, an indicator of the spermatogonial stages, was similar in the wild-type control, the *nos>tkv*^{CA}, and the *nos>dpp* backgrounds (Figure S3 and S4).

To check the effects of increased TGFβ signaling on the cell cycle phases during the TA, we enumerated CycE- and pH3-positive cysts, respectively, in the *nos>tkv*^{CA} background. We found a significant increase in the number of CycE-positive 8-cell cysts (Figure 2(B-B)) and a reduction in the percentage of CycE-positive 2-cell (28/100 = 28%, p = 0.012) and 4-cell (21/82 = 26%, p = 0.037) cysts in the *nos>tkv*^{CA} background as compared to the *nos>eGFP* control (67/152 = 44% 2-cell, 29/68 = 43% 4-cell). Also, the percentage of 8-cell cysts (26/44 = 59%, p = 0.003) was enhanced nearly two folds as compared to the control (19/64 = 30%). Together the result indicated that the TGFβ signaling could regulate the CycE-phase in a stage-specific manner during the TA. In mammalian systems, the BMP signaling controls the expression of CKIs (Cyclin-Dependent Kinase Inhibitors) of the Cip/Kip family, and thereby, regulates the extent of the CycE-Cdk2 activity [36–39]. Hence, increased BMP/TGFβ signaling in the early germline cells could enhance the CKI levels and terminate the G1 earlier than control. The extension of the CycE-phase at the 8-cell stage was, however, inexplicable.

To understand the significance of CycE modulation, we studied the mitosis rates in the *nos>tkv*^{CA} background. Although there was no significant difference in the distribution of the pH3 positive cysts (Figure 2(B-C)), the mitotic index of GBs was significantly higher, and that of the 4-cell cysts was significantly lower (Table 1). These results indicated that elevation of the BMP

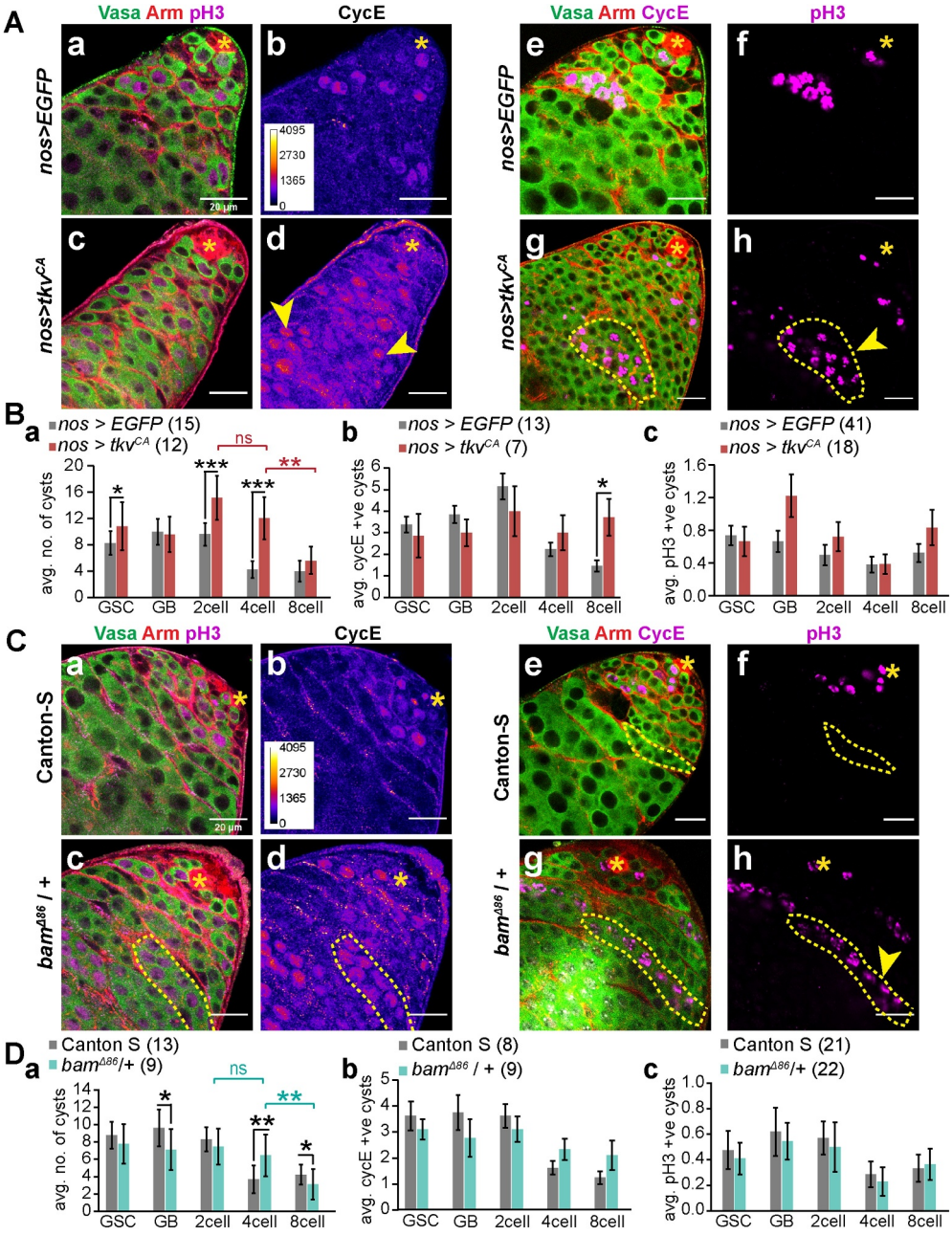

Figure 2. The effects of the upregulation of TGFβ signaling and partial loss of *bam* on the TA divisions. A) *nos>EGFP* (a, b, e, f) and *nos>tkv*^{CA} (c, d, g, h) testes stained with anti-vasa (Green), anti-armadillo (Red), and either with anti-CycE (a, b, c, d) or anti-pH3 (e, f, g, h). Dotted borders indicate >8-cell cyst, and asterisk marks the hub. (Scale bar ~20 µm). B) Histograms depict the number of spermatogonial cysts marked with – Vasa (average ± S. D., a), peak CycE staining (mean ± S. E. M., b), and pH3 (mean ± S. E. M., c) in the *nos>EGFP*, and *nos>tkv*^{CA} backgrounds. C) Canton-S (a, b, e, f) and *bam*$^{\Delta 86}$/+ (c, d, g, h) testes stained with anti-vasa (Green), anti-armadillo (Red), and either with anti-CycE (a, b, c, d) or anti-pH3 (e, f, g, h). Dotted borders indicate >8-cell cyst, and asterisk marks the hub. (Scale bar ~20 µm). D) Histograms depict the number of spermatogonial cysts in CantonS, and *bam*$^{\Delta 86}$/+ backgrounds marked with Vasa (mean ± SD, a), the peak CycE staining (mean ± SEM, b), and pH3 (mean ± SEM, c), respectively. The pair-wise significance of difference was estimated using the Mann-Whitney-U test (p-values are * <0.05, **<0.01, ***<0.001) and the sample numbers are as indicated on the graph.

signaling in GSCs and GBs leads to an acceleration of the first TA division and a slowdown of the third TA division, which resulted in alteration of the cyst distribution at the 2-cell, and 4-cell stages. A previous report in the *Drosophila* testis suggested that the TGFβ/BMP signaling is active in both the GSCs and GBs; however, its role in regulating the GSC and GB cell cycle was not

characterized [18]. The results described here suggest that BMP could differentially regulate the division rates of GBs and regulate the length of the G1 phase during TA.

The BMP signaling represses *bam* expression in the GSC and GB [18], and an increase in the Bam levels terminate the germline proliferation after the 8-cell stage [10]. Accordingly, we observed an accumulation of over-proliferating cysts containing more than 16 spermatogonia (arrows, Figure 2 (C-H)) in the $bam^{\Delta 86}$/+ testes. Also, similar to the $nos{>}tkv^{CA}$ background, the cyst distribution in $bam^{\Delta 86}$/+ background was altered. The number of 4-cell cysts was higher and comparable to that of the 2-cell cysts (Figure 2(D-A)). These results confirmed that the reduced accumulation of Bam protein could delay the progressive cell cycle remodeling during the TA. Although there was no significant change in the distribution of the CycE or pH3-stained cysts (Figure 2(D-B,C)), we noted that similar to $nos{>}tkv^{CA}$, the proportion of CycE-positive, 8-cell cysts (19/30 = 63%, p = 0.041) was significantly higher in the $bam^{\Delta 86}$/+ testis than those in the wild-type control (11/32 = 34%). The mitotic index of the 4-cell cysts was significantly lower (Table1).

Together, these results suggested that the Bam depletion slows down the third TA division, resulting in the alteration in the cyst distribution at the 4-cell and the 8-cell stages (Figure 2(D-A)). Moreover, the depletion of Bam also extends the CycE expression and consequently alters the G1 length at the 8-cell stage. Hence, Bam appeared to remodel the cell division rates at the 4-cell stage and the CycE/G1 length at the subsequent stage.

Bam overexpression is reported to progressively reduce GSCs and GBs without altering the relative distribution of 2-, 4- and 8-cell cysts [17]. We found that ectopic *hs-bam* expression, induced by short, heat-shock pulses, could reduce the number of GSCs ($\leq$4 in 3 out of 18) and GBs ($\leq$4 in 7 out of 18). Occasionally, we also noted 8-cell cysts close to the hub (Figure S5B). However, the phenotype was not consistent. Therefore, we did not proceed with the determination of CycE and pH3-positive cysts distribution. This observation, together with the previous report by 17, suggested that ectopic Bam overexpression could promote symmetric differentiation of the GSCs and possibly accelerate the GB divisions leading to a loss of GSCs.

CycE activity maintains the rates of GSC and GB divisions

Cyclin D and Cdk4/6 complex regulate the G1 phase, and the CycE/Cdk2 activity induces the G1/S transition. Therefore, to investigate the role G1 length regulation during the early TA divisions, we expressed $cycD^{dsRNA}$ and $cycE^{dsRNA}$ constructs, respectively, using *nosGal4vp16*. The cyst distribution was unaltered in the in $nos{>}cycD^{dsRNA}$ and nos>*cdk4* backgrounds (unpublished observation). The cell cycle is reported to continue in the absence of CycD/Cdk4 in *Drosophila* embryo [40, reviewed in 41]. Also, studies in the wing imaginal discs showed that the loss or overexpression of CycD/Cdk4 does not affect the G1 phase, but alters the length of the entire cell cycle [42]. Changing the cell cycle lengths of GSC and GB is expected to alter cyst distribution in subsequent stages. We found a similar phenotype in $nos{>}cycE^{dsRNA}$ background, which partly depleted the CycE levels in GSCs and GBs. There was a significant depletion in the number of CycE-positive GBs in the $nos{>}cycE^{dsRNA}$ background (Figure S6B) and a marginal decrease in the intensity of anti-CycE staining in GSCs and GBs (Figure S6 C), indicating that the RNAi partially reduced Cyclin E in the GSC and GB. The $nos{>}cycE^{dsRNA}$ testes had relatively fewer cysts in the TA region with visible gaps (Figure 3(A-B)), and we observed significant reductions in the number of GBs and 2-cell cysts (Figure 3(A-C)).

CycE levels regulate the extent of Cdk2 activity, which determines the G1 length. Therefore, to augment the CycE levels, we overexpressed a stable form of CycE, $cycE^{\Delta PEST}$, and to extend the CycE/Cdk2 activity, we expressed *dacapo* (*dap*, the p21 ^{CIP}/p27^{KIP1} ortholog) RNAi, using *nosGal4vp16* (*nos>*). The TA zone in $nos{>}cycE^{\Delta PEST}$ and $nos{>}dap^{dsRNA}$ testes appeared extended (Figure 3(B-A,B)). There was an increase in the 4-cell cysts in $nos{>}cycE^{\Delta PEST}$ background

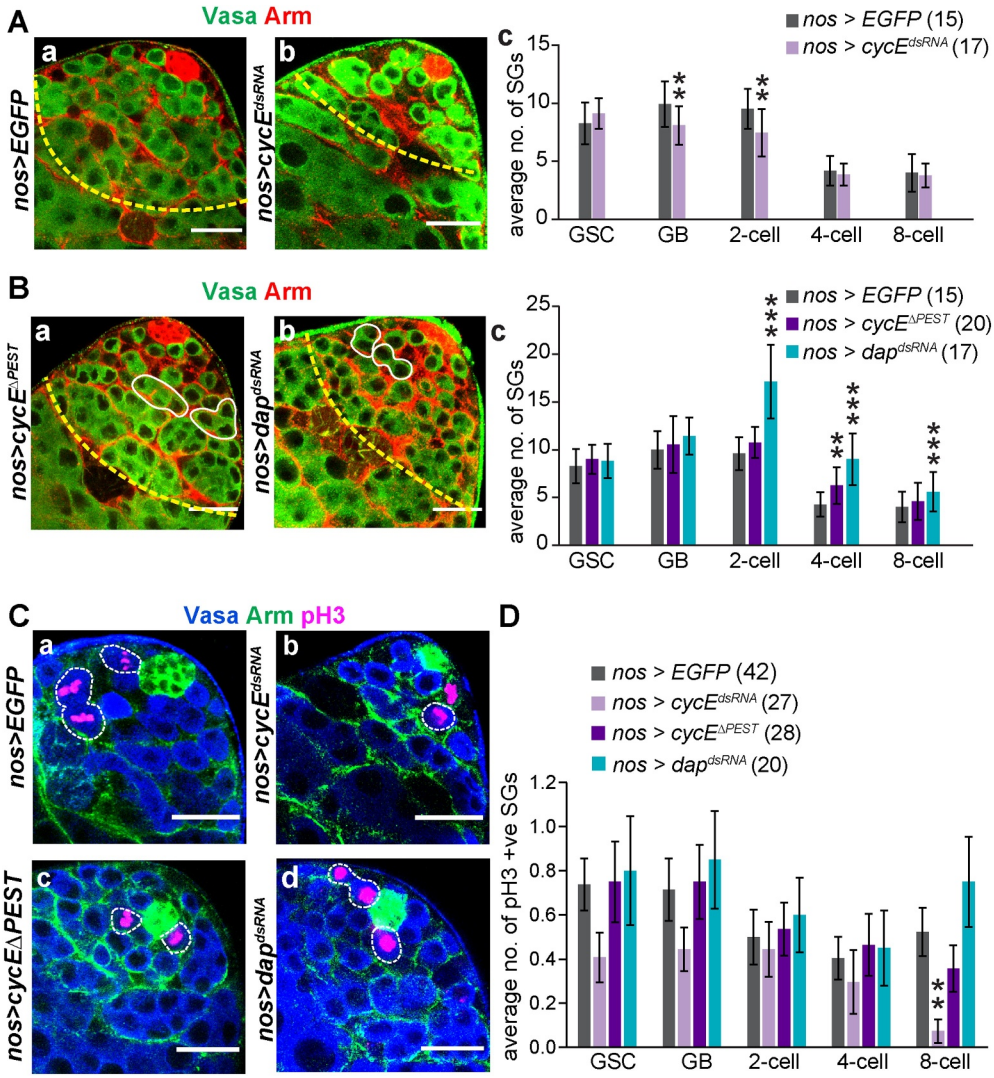

Figure 3. The perturbation of the CycE levels during the early stages altered the TA progression. A) *nos>EGFP* (a), and *nos>cycE*^{dsRNA} (b) testes stained with the Hoechst dye (blue), anti-Arm (Red), and anti-Vasa (green). The broken yellow line marks the edge of the TA region. (Scale bars ~20 µm). Histograms depict the stage-wise distribution (average ± SD) of GSCs and SGs (c). B) *nos>cycE*$^{\Delta PEST}$ (a), and *nos>dap*^{dsRNA} (b) testes stained with the Hoechst dye (blue), anti-Arm (Red), and anti-Vasa (green). The broken yellow line marks the edge of the TA region. (Scale bars ~20 µm). White borders indicated the accumulated 4-cell cysts in *nos>cycE*$^{\Delta PEST}$ testis and 2-cell cysts in *nos>dap*^{dsRNA} testis, respectively. Histograms depict the stage-wise distribution (average ± SD) of GSCs and SGs (c). C) Adult testes from *nos>EGFP* (a), *nos>cycE*^{dsRNA} (b), *nos>cycE*$^{\Delta PEST}$ (c), and *nos> dap*^{dsRNA} (d) backgrounds, stained with anti-Vasa (blue), anti-Arm (Red), and anti-phospho-histone3 (PH3 in magenta). PH3 positive stages are marked with a dotted outline. (scale bars ~20 µm). D) The histograms depict the stage-wise distribution (average ± S.E.) of pH3-positive G.S.C.s and SGs in the *nos>EGFP*, *nos>cycE*^{dsRNA}, *nos>cycE*$^{\Delta PEST}$, and *nos>dap*^{dsRNA} backgrounds. The pair-wise significance of difference was estimated using the Mann-Whitney U test (p-values are * <0.05, **<0.01, ***<0.001) and the sample numbers are as indicated on the histogram panels.

and a significant increase in 2, 4, and 8-cell cysts in the *nos>dap*^{dsRNA} background (Figure 3(B-C)). The stage-wise enumeration of cysts suggested that CycE/Cdk2 activity may regulate the cell cycle lengths of GSCs and GBs. A reduction of CycE/Cdk2 activity due to the *cycE* RNAi appeared to decrease the rates of GSC and GB divisions, and extended CycE/Cdk2 activity in *nos>cycE*$^{\Delta PEST}$ and *nos>dap*^{dsRNA} backgrounds accelerated the GSC and GB divisions resulting in the accumulation of 2-cell and 4-cell cysts.

A change in cell cycle length would alter the frequency of mitotic events. Therefore, we estimated the stage-specific distribution of cysts

stained with the pH3 antibody in the *nos>cycE*^{dsRNA}, *nos>cycE*$^{\Delta PEST}$, and *nos>dap*^{dsRNA} backgrounds (Figure 3(C)). In the *nos>cycE*^{dsRNA} testes, though the average GSC pool was comparable to that of the control (Figure 3(A-C), the average pH3-stained GSCs were less than 50% (Figure 3(D)). As a consequence, the GSC mitotic index was significantly reduced (11/246 = 4.5%; p-value = 0.04, Fisher's exact test) as compared to the control (31/321 = 9.7%). Although CycE level were not altered at the 8-cells stage in the *nos>cycE*^{dsRNA} testes, the average number of pH3-positive cysts at the 8-cell stage was significantly reduced (p-value = 0.002, Mann Whitney U test) (Figure 3(D)). Also, there was a marginal increase in the pH3-positive cysts at the 8-cell stage in *nos>dap*^{dsRNA} testes (Figure 3(D)). These results demonstrated that the CycE activity is particularly crucial for maintaining the division rates of GSCs and that of the 8-cell spermatogonia. The alterations of the cell division rates during the early TA stages, however, did not affect the cyst differentiation (Figure S7).

Cdk1 activity maintains the GSC and regulates the rates of GSC and GB divisions

Cyclin B and Cdk1 complex regulate the G2 phase. In the *nos>cdk1*^{dsRNA} background, the pool of GB was significantly reduced, but the GSC pool remained unaltered, suggesting that the loss of Cdk1 could slow down the rates of GSC divisions (Figure 4(A-B)). Next, we used a previously characterized *cdc25/string* (*stg*) RNAi [25] and overexpression of *wee1* to deplete the Cdk1 activity (Figure 4(B)). We also overexpressed *stg* to augment Cdk1 activity in the GSCs and GBs (Figure 4(C)). 25, showed that that Stg is required for the GSC maintenance. Consistent with this report, we observed a significant reduction in the GSC number in *nos>stg*^{dsRNA} background (Figure 4(B-C)). We also noticed a significant depletion of the GSC pool in the *nos>wee1* background (Figure 4(B-C)). Together, these results suggested that the levels of Cdk1 activity may be critical for GSC maintenance. Also, the *nos>stg* overexpression significantly increased the number of 2, 4, 8, and 16-cell cyst (Figure 4(C-B)), indicating that the Cdk1 activity regulates the rates of GSC and subsequent TA divisions as well.

Consistent with the above conjecture, we observed ~50% reduction in the average number of pH3-positive GSCs in both the *nos>cdk1*^{dsRNA} (p-value = 0.065, Mann Whitney U test) and *nos>stg*^{dsRNA} (p-value = 0.056, Mann Whitney U test) backgrounds, and ~2-fold increase in the average number of pH3-positive GSCs, GBs and 2-cell cysts in the *nos>stg* background (Figure 4(E)). Since the average number of GSC and GBs were not altered in the *nos>stg* background (Figure 4(C-B)), we concluded that the increased Cdk1 activity during the early stages speed-up the rates of GSC and GB divisions. Similar to the results in CycE perturbation, the alteration in Cdk1 activity did not affect the meiosis and subsequent differentiation (Figure S7).

Inexplicably though, we found a significant increase in the number of pH3-positive GSCs and a marginal increase in the average number of pH3-positive cysts during the early stages in the *nos>wee1* background (Figure 4(E)). Histone 3 phosphorylation begins in late G2 [43,44]. Hence, the increase could be attributed to a longer G2 and/or mitotic prophase. Indeed, a previous study in the human cell culture system has shown that wee1 overexpression leads to a slow Cdk1 activation and longer mitosis [45]. The loss of CDK1, on the other hand, would arrest the induction of M-phase altogether and reduce the number of pH3-stained cysts. Together, these results also indicated that up to 2x modulations of the rates of GSC and GB divisions does not alter the number of TA divisions and subsequent differentiation program.

CycE and CDK1 levels control cell cycle progression at the 8-cell stage

Therefore, to study the role of the cell cycle phase regulators during the second half of TA, we expressed the *cycE, stg, dap*, and *cdk1* RNAi, as

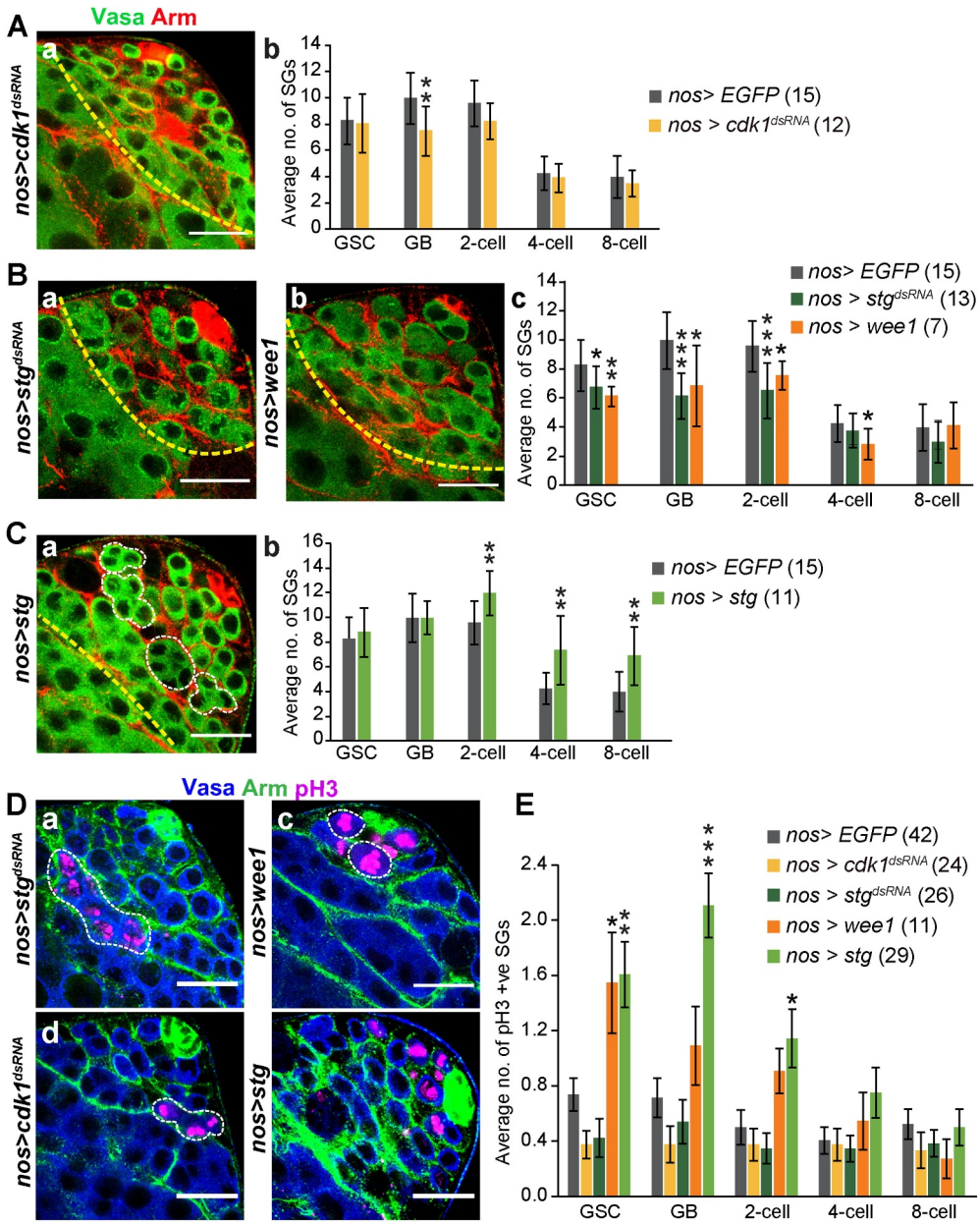

Figure 4. The perturbation of the CDK1 activity during the early stages affected the GSC maintenance and altered the TA progression. A) A *nos>cdk1*^{dsRNA} testis stained with the Hoechst dye (blue), anti-Arm (Red), and anti-Vasa (green), shows a shrunken apical tip with fewer spermatogonial cysts (a, Scale ~20 µm). The TA region is marked with a yellow dotted line. Histograms depict the stage-wise distribution (average ± SD) of GSCs and SGs in different genetic backgrounds (b). **B)** Adult testis from *nos>stg*^{dsRNA} (a), and *nos>wee1* (b) flies, stained with the Hoechst dye (blue), anti-Arm (Red), and anti-Vasa (green), show shrunken apical tip with fewer Spermatogonial cysts as compared to control. (Scale bars ~20 µm). Germline TA region is marked with a yellow dotted line. Histograms depict the stage-wise distribution (average ± SD) of GSCs and SGs in different genetic backgrounds (c). **(C)** *nos>stg*(a) testis stained with the Hoechst dye (blue), anti-Arm (Red), and anti-Vasa (green), show shrunken apical tip with fewer spermatogonial cysts as compared to control. (Scale bars ~20 µm). Germline TA region is marked with a yellow dotted line. The 4-cell SGs in is highlighted with white dotted lines. Histograms depict the stage-wise distribution (average ± SD) of GSCs and SGs (b). (d) Testes from *nos>stg*^{dsRNA} (b), *nos>wee1* (c), *nos>cdk1*^{dsRNA} (d) and *nos>stg* (e) flies, stained with anti-Vasa (blue), anti-Arm (Red), and anti-phospho-histone3 (PH3 in magenta). (Scale bars ~20 µm). PH3 positive stages are marked with a dotted outline. (E) The histograms depict the stage-wise distribution (average ± SE) of PH3-positive SGs in *nos>EGFP*, *nos>stg*^{dsRNA}, *nos>wee1*, *nos>Cdk1*^{dsRNA}, and *nos>stg* backgrounds. The pair-wise significance of difference was estimated using the Mann-Whitney U test (p-values are * <0.05, **<0.01, ***<0.001) and the sample numbers are as indicated on the histogram panels.

well as *wee1* and *stg* transgenes, respectively, using 2x*bamGal4*, and examined the effect of these perturbations on the spermatocyte population by counting all cysts in the testis apex within ~135 μm from the hub. This area consists of the GSCs, the TA stages, and the spermatocyte pool, including the S3-stage spermatocytes [28].

The *bam>cycE*^{dsRNA} expression depleted the number of CycE-positive 4, 8, and 16-cell cysts (Figure 5(A,B)). Also, the intensity of anti-CycE staining was significantly reduced in 4, 8, and 16-cell spermatogonia (Figure 5(C)). The *cycE*^{dsRNA} expression led to an increase in the GB pool, and a substantial accumulation of the 4-cell and 8-cell cysts (Figure 5(D)), indicating a slowdown of the TA divisions at the 4-cell and 8-cell stage. On the other hand, the expression of *bam>cycE*$^{\Delta PEST}$ and *bam>dap*^{dsRNA} did not affect the cyst distribution and subsequent differentiation (Figure 5(D), S8 and S9). These results suggested that CycE is required for cell cycle progression at the 4 and 8-cell stages, but the regulation of CycE/Cdk2 activity by Dap is limited to the early TA stages.

In both the *cdk1* RNAi and *wee1* overexpression backgrounds, the number of 4-cell cysts was increased by ~2-fold, and the testes were filled with only 8-cell cysts (Figure 5(E,F)), indicating that depletion in Cdk1 activity could slow down the third TA division, and arrest the TA at the 8-cell stage. As expected, the expression of *stg*^{dsRNA} transgene in 4–16 cell stages did not alter the cyst distributions and subsequent differentiation (figfigure 5(F)), demonstrating that the Cdc25/Stg function is limited to the GSCs and early TA stages. Consistent with the previous report [10], the *bam>stg* overexpression depleted the pool of 16-cell cysts and a new pool of 32-cell cysts consisting of spermatogonia-like cells was found, indicating that the spermatogonial cells at the 16-cell stage undergo one extra round of mitotic division upon overactivation of Cdk1 before differentiation (figure 5(F)). Together, these two set of results suggested that the regulation of Cdk1 activity after the second TA divisions is essential for limiting the number of amplifying divisions.

Cell cycle phase modulation induces premature induction of meiosis at the 8-cell stage

As spermatocytes enter meiotic prophase, the cells increase in volume by about 25 fold [12]. Therefore, to investigate whether the cysts arrested at the 8-cell stage in the *cycE*and *cdk1* RNAi backgrounds enter meiosis, we measured the nuclear area of germline cells at 4-cell, 8-cell and spermatocyte stages in wild-type testes. We selected the cysts carrying S3-like spermatocytes in the respective RNAi backgrounds (Figure 5(G)) and measured the max nucleus area (Figure 5(H)). We found that a good number of the 8-cell cysts (65 out of 140 cysts) in *bam>cycE*^{dsRNA} (Figure 5(H)), and almost all the accumulated 8-cell cysts in *bam>cdk1*^{dsRNA} testes had nuclear sizes similar to that of the S3-stage spermatocytes found in the wild-type control (Figure 5(H)). Moreover, we also found some occasional 4-cell cysts (5 out of 61 cysts) in *bam>cdk1*^{dsRNA} background with a nuclear size similar to that of the S3-stage spermatocytes in control testes (Figure 5(H)). These results suggested that the cell cycle arrest at the 8-cell stage due to the *cycE* and *cdk1* knockdown could lead to premature entry into meiosis. The results described here further suggest that CycE and the levels of Cdk1 activity determine the cell cycle length during the penultimate TA division, which regulates the induction of meiosis.

After the fourth TA division, all the spermatogonia in a 16-cell cyst proceed through the S-phase and an extended G2 [46, Reviewed in 12]. This premeiotic G2 extension is mediated by a Cdk1 inhibitory kinase [47], and the expression of twine (CDC25 homolog) promotes Cdk1 activity and entry into meiosis [48]. A previous report also indicated that *cdc2 (cdk1)* is required for the meiosis in the *Drosophila* testis [49]. Consistent with these results, we did not observe any mature sperm in *bam>cdk1*^{dsRNA} background (Figure S8), indicating that cdk1 is indispensable for the meiotic division and further differentiation. Whereas we observed several clusters of post-meiotic, spermatid nuclei, bundles of sperm tails, and sperm nuclei in the seminal vesicle in the *bam>cycE*^{dsRNA} testes

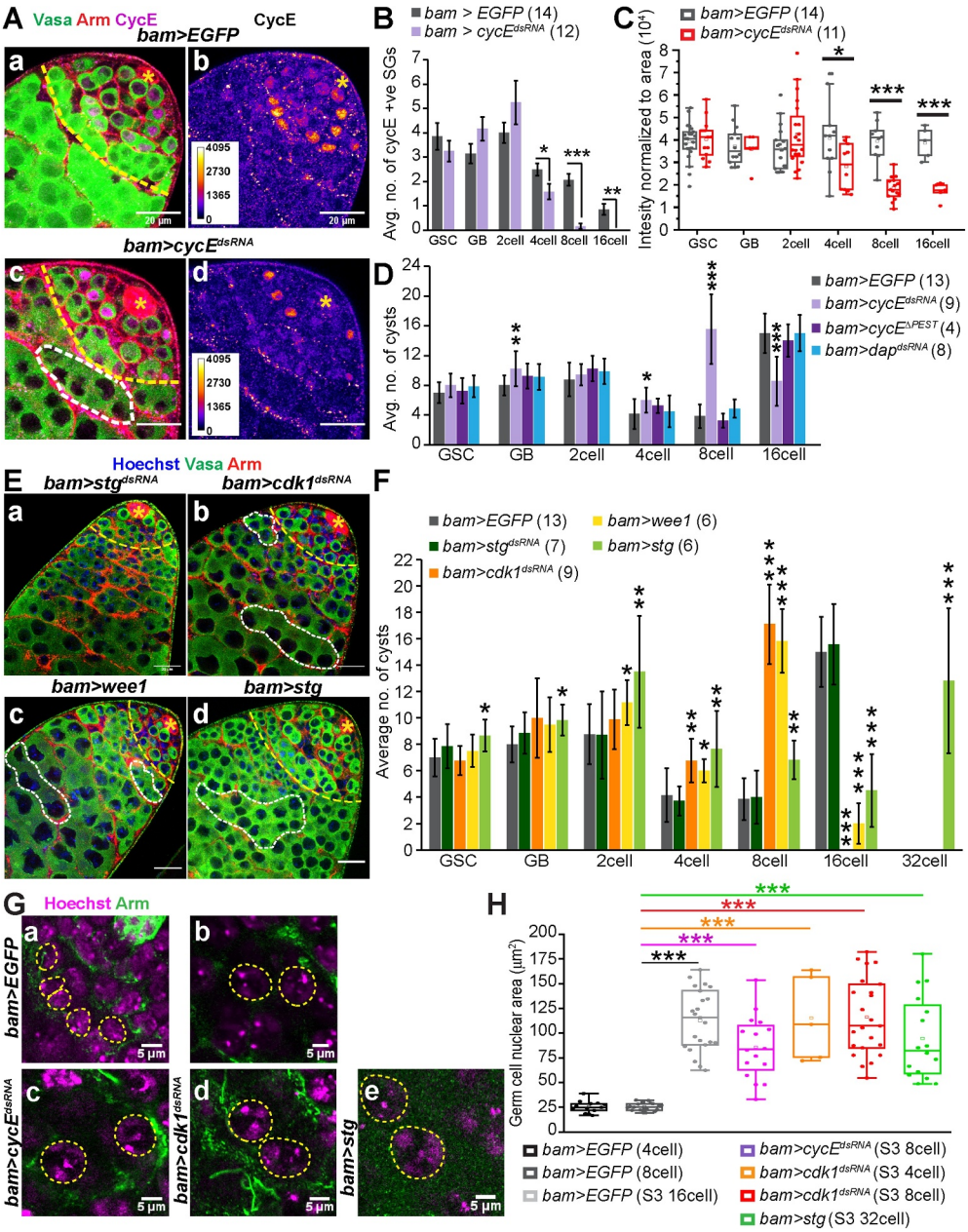

Figure 5. RNAi of cycE and cdk1 during the later stages affect TA divisions at the 8-cell stage. A) Apical tip of an adult testis from bam>EGFP (a, b) and bam>cycEdsRNA (c, d) backgrounds stained with anti-Vasa (green), anti-Arm (Red), and anti-CycE (magenta). Asterix marks the hub. B) Histograms depict the stage-wise estimation of the intensity of CycE staining (average ± SD) in bam>EGFP and bam>cycEdsRNA backgrounds. C) Box plot depicts the estimation of the CycE-positive cysts in bam>EGFP and bam>cycEdsRNA backgrounds. D) Histograms depict the stage-wise distribution (averages ± SD) of cysts in different genetic backgrounds. E) Apical tip of testes from bam>stgdsRNA (a), bam>Cdk1dsRNA (b), bam>wee1 (c) and bam>stg (d) backgrounds stained with the Hoechst dye (blue), anti-Vasa (green), anti-Arm (Red). Yellow dotted lines mark the TA zone and the white dotted outlines indicate 8-cell spermatogonial cysts beyond the TA zone. (scale bars ~20 µm). F) Histograms depict the stage-wise distribution (averages ± SD) of cysts in different genetic backgrounds. G) Cropped images of bam>EGFP (a, b), bam>cycEdsRNA (c) and bam>cdk1dsRNA (d) and bam>stg (e) testes stained with Hoechst (magenta) and anti-armadillo (Green). Yellow dotted lines mark the 8-cell spermatogonial nuclei (a), 16-cell S3 spermatocyte (b) in control, 8-cell S3-like spermatocytes in the bam>cycEdsRNA (c) and bam>cdk1dsRNA (d), and a 32-cell S3-like spermatocytes in the bam>stg (e) backgrounds. (scale bars ~5 µm). H) The box plots indicate nuclear diameters of the 4- and 8-cell spermatogonia, and the 4-, 8- and 16-cell, S3-stage spermatocytes in the bam>EGFP, bam>cycEdsRNA, bam>Cdk1dsRNA, and bam>stg backgrounds. The pair-wise significance of difference was estimated using the Mann-Whitney-U test (p-values are * <0.05, **<0.01, ***<0.001) and the sample numbers are as indicated on the graph.

(Figure S9), indicating that loss of CycE is unlikely to arrest meiosis and spermatid differentiation fully.

Discussion

The termination of TA divisions is one of the critical aspects of tissue homeostasis. Previous studies suggested that independent regulation of cell cycle length and a 'differentiation clock" determines the extent of the TA. Here, we show that the cell cycle structure, particularly the CycE and CycB-positive phases, is progressively altered during the amplification divisions of the *Drosophila* male germline lineage (Figure 6(A)). An ongoing study in the lab revealed that the duration of M-phase marked by the pH3 staining does not vary during the TA (Gadre, Mazumdar, and Ray, unpublished data). Therefore, we used the frequency of pH3-stained cysts to normalize the occurrences of the other cell cycle phase markers at each stage (Figure 6). It suggests that the relative cell cycle length increases during the second TA division and then shortens in the subsequent stages. This analysis also illustrated that the G1 length increases until the second TA division, then shortens during the next two divisions. The G1 length is the shortest during the penultimate mitotic division before the onset of meiosis. To reconcile the apparent change in the relative cell cycle length with the step increase of mitotic index at the 4-cell stage, we hypothesize that the GSCs and GBs could be spending a considerable time at a quiescent state (G0) during their life cycle. The G0 stage could be contracted at the 2-cell stage at the expense of an expanding cell cycle length and possibly abolished at the 4-cell stage.

Cell cycle acceleration at the 4-cell stage coincides with the Bam expression, which is repressed by the TGF-β signaling in GSC and GB. Activation of the TGFβ signaling, which includes the BMP class, is known to induce G1 arrest via inhibition of CycE/Cdk2 activity [50–52]. Here, we show that the antagonistic actions of BMP signaling and Bam regulate the division rate at the 4-cell stage, as well as the extent of the CycE phase and the cell cycle structure during the TA in the *Drosophila* testis (Figure 6(B)). An ectopic gain of TGF-β signaling and partial loss of Bam significantly reduced the mitotic index of the 4-cell stage. It also extended the persistence of CycE-

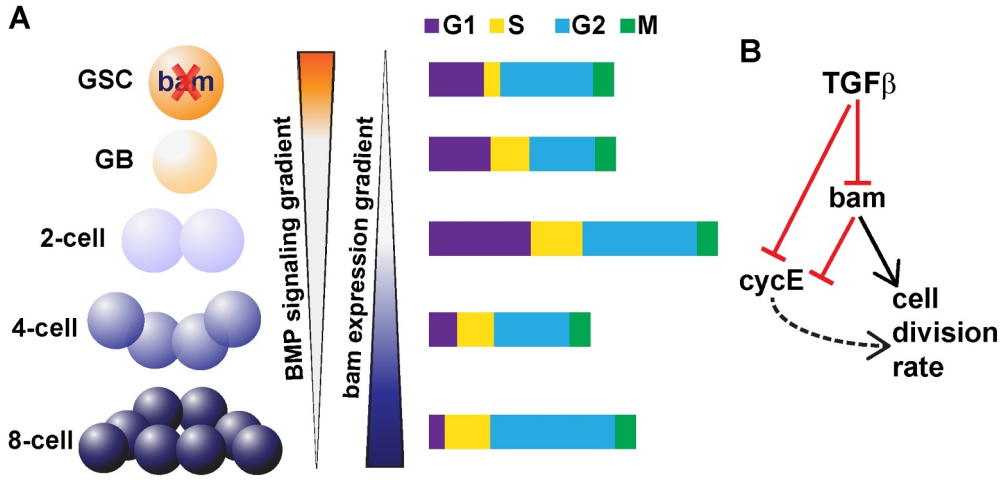

Figure 6. Regulation of the germline cell cycle during TA. A) Schematic illustrates progressive restructuring of the cell cycle phases during the transit amplification of male germline in Drosophila. Colored bars represent the extent of cell cycle phases relative to the M-phase duration, which is expected to remain constant throughout the TA. It is calculated based on the data presented in Figure 1 G and H. B) The schematic illustrates the role of TGFβ signaling and Bam in the regulation of germline cell cycle during the TA Previous studies have shown that TGFβ signaling represses bam expression in the GSCs [18, 19]. In this study, we showed that Bam function, potentially antagonized by the TGFβ signaling, regulates the cell division rates at the 4-cell stage and the extent of CycE expression at the 8-cell stage.

phase at the 8-cell stage when the Bam expression reaches its peak. Therefore, we conclude that Bam might also regulate CycE activity.

A short G1 phase is associated with stem cell identity [reviewed in 53, 54]. Previous studies have suggested that inhibition of CycE induces stem cell differentiation, whereas the extension of CycE delays it [55–57]. We found that the CycE activity is particularly necessary to regulate the division rates of GSC and the TA stages. However, a significant loss of CycE at the 4- and 8-cell stage did not arrest the TA. CycA induces G1/S transition in the absence of CycE in the *Drosophila* embryo [58]. Although there was no discernable change in the persistence of CycA-phase at the 4 and 8-cell stage, we postulate that in the reduced CycE background, the CycA activity could continue the TA at the 8-cell stage with lower efficiency, which resulted in the accumulation of 4 and 8-cell cysts in the $bam{>}cycE^{dsRNA}$ testis.

In the *C. elegans* germline, constant activation of CycE/CDK2 drives cell divisions in the TA-like proliferative stage, bypassing the G1 phase, and loss of CycE induces premature entry into meiosis [59]. We found that the loss of CycE could induce premature meiosis only at the 8-cells stage. Also, the extension of CycE levels and CycE/Cdk2 activity due to the overexpression of $cycE^{\Delta PEST}$ and dap RNAi in the GSCs and GBs possibly increased the proliferation rates, causing the accumulation of cysts at the subsequent stages. However, similar perturbations at the 4- and 8-cell stages did not affect the TA. It may suggest an independent and partly redundant mechanism could terminate G1 in the extended CycE background during the latter half of TA.

The *Drosophila* GSCs have short G1, and longer G2 phases [21,24,33], and the G2 regulation is critical for GSC maintenance [25]. Consistent with these reports, we found that the number of CycE-positive GSCs in the testis is less than that marked by CycB, and the Cdk1 activity levels maintain GSCs. Also, the proportion of CycB stained cysts increases steadily with each TA division and remains high until the 8-cell stage. The genetic analysis further suggested that the Cdk1 activity is likely to be critically balanced at the 4- and 8-cell stages to ensure the TA progression. Loss of Cdk1 function arrested the TA, and ectopic overactivation extended the TA. Altogether the results suggest that G2 regulation through a calibration of CdK1 activity at different stages is essential for the GSC maintenance, the progression of the final TA division, and the induction of meiosis in the male germline. In other words, the relative extension of the G2 phase appeared to determine the cell cycle structure and the differentiation fate of the progeny cells in the male germline of *Drosophila*.

Previous studies showed that along with the niche, the TA progenitors also signal the stem cells and regulate their divisions in both the transient and continuously regenerative tissues [60,61]. Multiple studies have also observed that early spermatogonia reassociate with the niche to replenish GSCs in the *Drosophila* testis [17,62,63]. Interestingly, we noted that the knockdown of CycE and Cdk1 in GSCs and early-stage cysts, respectively, led to a depletion of only the GB, 2- and 4-cell cysts without affecting the later stages. This result suggests the existence of a feed-forward mechanism that could alter the rates of subsequent TA divisions to maintain the pool of transit-amplifying cysts in response to a shortage in the supply of early cysts, highlighting the complexity of the regulation of homeostasis in stem cell and TA systems.

Acknowledgments

We thank Benny Shilo, Talila Volk, and Eli Arama, Weismann Institute, Israel; Kenneth Irvine, Waksman Institute of Microbiology, New Jersey, USA; Dorothea Godt, Univ. Toronto, Canada; Lynn Cooley, Yale School of Medicine, Connecticut, USA; Dennis McKearin; Pradip Sinha, IIT Kanpur, India; Bloomington Stock Center, Indiana, USA; Vienna Drosophila Resource Center, Austria; and Developmental Studies Hybridoma Bank, Iowa, USA; for fly stocks and other reagents. A special thanks to Prof. Shilo for critical comments and suggestions throughout the study.

Author's contribution

PG: Cyst distribution, pH3 distribution, and germ cell death distribution in control and cell cycle perturbed genotypes. PG, SC, and BV: Cyst distribution in wild type and cell cycle marker frequency. PG, SC, and KR: data analysis. PG and KR: figures composition and manuscript writing. All the authors contributed to evolving the concept.

Disclosure statement

The authors have no competing interest in the publication of the results.

Funding

KR, PG, and BV were supported by the intramural grant of Dept. of Atomic Energy (DAE), Government of India, to TIFR. SC was supported by the Department of Biotechnology (DBT), Government of India. The study was partly supported by the DBT grant BT/PR/4585/Med/31/155/2012 (dated 28 September 2012) and in part by the DAE, TIFR grant 12-R&D-TFR-5.10-100; Department of Atomic Energy, Government of India.

ORCID

Purna Gadre http://orcid.org/0000-0002-3255-6295
Shambhabi Chatterjee http://orcid.org/0000-0001-5978-3562
Krishanu Ray http://orcid.org/0000-0001-6406-3199

References

[1] Lajtha LG. Stem cell concepts. Differentiation. 1979;14 (1–2):23–34.
[2] Potten CS, Loeffler M. Stem cells: attributes, cycles, spirals, pitfalls and uncertainties. Lessons for and from the crypt. Development. 1990;110:1001–1020.
[3] Rangel-huerta E, Maldonado E. Transit-Amplifying Cells in the Fast Lane from Stem Cells towards Differentiation. Stem Cells Int. 2017;2017:1–10.
[4] Lange C, Calegari F. Cdks and cyclins link G1 length and differentiation of embryonic, neural and hematopoietic stem cells. Cell Cycle. 2010;9 (10):1893–1900.
[5] Lacomme M, Liaubet L, Pituello F, et al. NEUROG2 Drives Cell Cycle Exit of Neuronal Precursors by Specifically Repressing a Subset of Cyclins Acting at the G1 and S Phases of the Cell Cycle. Mol Cell Biol. 2012;32(13):2596–2607.
[6] Siatecka M, Lohmann F, Bao S, et al. EKLF directly activates the p21WAF1/CIP1 gene by proximal promoter and novel intronic regulatory regions during erythroid differentiation. Mol Cell Biol. 2010;11:2811–2822.
[7] Ruijtenberg S, den Heuvel S. Coordinating cell proliferation and differentiation: antagonism between cell cycle regulators and cell type-specific gene expression. Cell Cycle. 2016;15:196–212.
[8] Gao FB, Durand B, Raff M. Oligodendrocyte precursor cells count time but not cell divisions before differentiation. Curr Biol. 1997;7(2):152–155.
[9] Dugas JC, Ibrahim A, Barres BA. A Crucial Role for $p57^{Kip2}$ in the Intracellular Timer that Controls Oligodendrocyte Differentiation. J Neurosci. 2007;27 (23):6185–6196.
[10] Insco ML, Leon A, Tam CH, et al. Accumulation of a differentiation regulator specifies transit amplifying division number in an adult stem cell lineage. Proc Natl Acad Sci U S A. 2009;106:22311–22316.
[11] Hardy RW, Tokuyasu KT, Lindsley DL, et al. The germinal proliferation center in the testis of Drosophila melanogaster. J Ultrastruct Res. 1979;69:180–190.
[12] Fuller MT. Genetic control of cell proliferation and differentiation in Drosophila spermatogenesis. Semin Cell Dev Biol. 1998;9:433–444.
[13] Monk AC, Siddall NA, Volk T, et al. HOW is required for stem cell maintenance in the Drosophila testis and for the onset of transit-amplifying divisions. Cell Stem Cell. 2010;6(4):348–360.
[14] Ji S, Li C, Hu L, et al. Bam-dependent deubiquitinase complex can disrupt germline stem cell maintenance by targeting cyclin A. Proc Natl Acad Sci. 2017;114:6316–6321.
[15] Li Y, Minor NT, Park JK, et al. Bam and Bgcn antagonize Nanos-dependent germline stem cell maintenance. Proc Natl Acad Sci U S A. 2009;106:9304–9309.
[16] Shen R, Xie T. Stem cell self-renewal versus differentiation: tumor suppressor Mei-P26 and miRNAs control the balance. Cell Res. 2008;18:713–715.
[17] Sheng RX, Brawley CM, Matunis EL. Dedifferentiating Spermatogonia Outcompete Somatic Stem Cells for Niche Occupancy in the Drosophila Testis. Cell Stem Cell. 2009;5:191–203.
[18] Kawase E, Wong MD, Ding BC, et al. Gbb/Bmp signaling is essential for maintaining germline stem cells and for repressing bam transcription in the Drosophila testis. Development. 2004;131:1365–1375.
[19] Chang Y-J, Pi H, Hsieh -C-C, et al. Smurf-mediated differential proteolysis generates dynamic BMP signaling in germline stem cells during *Drosophila* testis development. Dev Biol. 2013;383:106–120.
[20] Hinnant TD, Alvarez AA, Ables ET. Temporal remodeling of the cell cycle accompanies differentiation in the Drosophila germline. Dev Biol. 2017;429:118–131.
[21] Ables ET, Drummond-Barbosa D. Cyclin E controls Drosophila female germline stem cell maintenance independently of its role in proliferation by modulating responsiveness to niche signals. Development. 2013;140:530–540.

[22] Wang Z, Lin H. The division of *Drosophila* germline stem cells and their precursors requires a specific cyclin. Curr Biol. 2005;15:328–333.
[23] Liu T, Wang Q, Li W, et al. Gcn5 determines the fate of Drosophila germline stem cells through degradation of Cyclin A. Faseb J. 2017;5:2185–2194.
[24] Hsu HJ, LaFever L, Drummond-Barbosa D. Diet controls normal and tumorous germline stem cells via insulin-dependent and -independent mechanisms in Drosophila. Dev Biol. 2008;313:700–712.
[25] Inaba M, Yuan H, Yamashita YM. String (Cdc25) regulates stem cell maintenance, proliferation and aging in Drosophila testis. Development. 2011;138:5079–5086.
[26] Joti P, Ghosh-Roy A, Ray K. Dynein light chain 1 functions in somatic cyst cells regulate spermatogonial divisions in *Drosophila*.. Sci Rep. 2011;1:173.
[27] Gupta S, Varshney B, Chatterjee S, et al. Somatic ERK activation during transit amplification is essential for maintaining the synchrony of germline divisions in Drosophila testis. Open Biol. 2018;8(7):180033.
[28] Gupta S, Ray K. Somatic PI3K activity regulates transition to the spermatocyte stages in Drosophila testis. J Biosci. 2017;42:1–13.
[29] Brantley SE, Fuller MT. Somatic support cells regulate germ cell survival through the Baz/aPKC/Par6 complex. Development. 2019;146:dev169342.
[30] Yacobi-Sharon K, Namdar Y, Arama E. Alternative Germ Cell Death Pathway in Drosophila Involves HtrA2/Omi, Lysosomes, and a Caspase-9 Counterpart. Dev Cell. 2013;25(1):29–42.
[31] Yang H, Yamashita YM. The regulated elimination of transit-amplifying cells preserves tissue homeostasis during protein starvation in Drosophila testis. Development. 2015;142:1756–1766.
[32] Chiang AC-Y, Yang H, Yamashita YM. spict, a cyst cell-specific gene, regulates starvation-induced spermatogonial cell death in the Drosophila testis. Sci Rep. 2017;7:40245.
[33] Sheng XR, Matunis E. Live imaging of the Drosophila spermatogonial stem cell niche reveals novel mechanisms regulating germline stem cell output. Development. 2011;138(16):3367–3376.
[34] Zielke N, Korzelius J, van Straaten M, et al. Fly-FUCCI: a versatile tool for studying cell proliferation in complex tissues. Cell Rep. 2014;7(2):588–598.
[35] Xia L, Jia S, Huang S, et al. The Fused/Smurf complex controls the fate of Drosophila germline stem cells by generating a gradient BMP response. Cell. 2010;143 (6):978–990.
[36] Ghosh-Choudhury N, Ghosh-Choudhury G, Celeste A, et al. Bone morphogenetic protein-2 induces cyclin kinase inhibitor p21 and hypophosphorylation of retinoblastoma protein in estradiol-treated MCF-7 human breast cancer cells. Biochim Biophys Acta. 2000;1497(2):186–196.
[37] Sharov AA, Sharova TY, Mardaryev AN, et al. Bone morphogenetic protein signaling regulates the size of hair follicles and modulates the expression of cell cycle-associated genes. Proc Natl Acad Sci USA. 2006;103(48):18166–18171.
[38] Gosselet FP, Magnaldo T, Culerrier RM, et al. BMP2 and BMP6 control p57 (Kip2) expression and cell growth arrest/terminal differentiation in normal primary human epidermal keratinocytes. Cell Signal. 2007;1 9(4):731–739.
[39] Chang SF, Chang TK, Peng HH, et al. BMP-4 induction of arrest and differentiation of osteoblast-like cells via p21 CIP1 and p27 KIP1 regulation. Mol Endocrinol. 2009;23(11):1827–1838.
[40] Meyer CA, Jacobs HW, Datar SA, et al. Drosophila Cdk4 is required for normal growth and is dispensable for cell cycle progression. Embo J. 2000;19 (17):4533–4542.
[41] Foley E, Sprenger F. Cyclins: growing pains for Drosophila. Curr Biol. 2000;10(18):R665–7.
[42] Datar SA. The Drosophila cyclin D-Cdk4 complex promotes cellular growth. Embo J. 2000;19(17):4543–4554.
[43] Hendzel MJ, Wei Y, Mancini MA, et al. Mitosis-specific phosphorylation of histone H3 initiates primarily within pericentromeric heterochromatin during G2 and spreads in an ordered fashion coincident with mitotic chromosome condensation. Chromosoma. 1997;106(6):348–360.
[44] Juan G, Traganos F, James WM, et al. Histone H3 phosphorylation and expression of cyclins A and B1 measured in individual cells during their progression through G2 and mitosis. Cytometry. 1998;32:71–77.
[45] Araujo AR, Gelens L, Sheriff RSM, et al. Positive Feedback Keeps Duration of Mitosis Temporally Insulated from Upstream Cell-Cycle Events. Mol Cell. 2016;64:362–375.
[46] Lindsley DT, Tokuyasu KT. Spermatogenesis. In: Ashburner M, Wright TRF, editors. The Genetics and Biology of Drosophila. Vol. 2d. London: Academic Press; 1980. p. 225–294.
[47] Varadarajan R, Ayeni J, Jin Z, et al. Myt1 inhibition of Cyclin A/Cdk1 is essential for fusome integrity and premeiotic centriole engagement in Drosophila spermatocytes. Mol Biol Cell. 2016;27(13):2051–2063.
[48] Courtot C, Fankhauser C, Simanis V, et al. The Drosophila cdc25 homolog twine is required for meiosis. Development. 1992;116:405–416.
[49] Sigrist S, Ried G, Lehner CF. Dmcdc2 kinase is required for both meiotic divisions during Drosophila spermatogenesis and is activated by the Twine/cdc25 phosphatase. 1995;53:247–260. .
[50] Koff A, Ohtsuki M, Polyak K, et al. Negative regulation of G1 in mammalian cells: inhibition of cyclin

E-dependent kinase by TGF-beta. Science. 1993;260 (5107):536–539.
[51] Reynisdóttir I, Polyak K, Iavarone A, et al. Kip/Cip and Ink4 Cdk inhibitors cooperate to induce cell cycle arrest in response to TGF-beta. Genes Dev. 1995;9:1831–1845.
[52] Nagahara H, Ezhevsky SA, Vocero-Akbani AM, et al. Transforming growth factor beta targeted inactivation of cyclin E: cyclin-dependent kinase 2 (Cdk2) complexes by inhibition of Cdk2 activating kinase activity. Proc Natl Acad Sci U S A. 1999;96(26):14961–14966.
[53] Dalton S. Linking the Cell Cycle to Cell Fate Decisions. Trends Cell Biol. 2015;25(10):592–600.
[54] Boward B, Wu T, Dalton S. Concise Review: control of Cell Fate through Cell Cycle and Pluripotency Networks. Stem Cells. 2016;34(6):1427–1436.
[55] Coronado D, Godet M, Bourillot PY, et al. A short G1 phase is an intrinsic determinant of naïve embryonic stem cell pluripotency. Stem Cell Res. 2013;10 (1):118–131.
[56] Rai M, Katti P, Nongthomba U. Spatio-temporal coordination of cell cycle exit, fusion and differentiation of adult muscle precursors by Drosophila Erect wing (Ewg). Mech Dev. 2016;141:109–118.
[57] Liu L, Michowski W, Inuzuka H, et al. G1 cyclins link proliferation, pluripotency and differentiation of embryonic stem cells. Nat Cell Biol. 2017;19:177–188.
[58] Sprenger F, Yakubovich N, O'Farrell PH. S-phase function of Drosophila cyclin A and its downregulation in G1 phase. Curr Biol. 1997;7(7):488–499.
[59] Fox PM, Vought VE, Hanazawa M, et al. Cyclin E and CDK-2 regulate proliferative cell fate and cell cycle progression in the C. elegans germline. Development. 2011;138(11):2223–2234.
[60] Rezza A, Wang Z, Sennett R, et al. Signaling Networks among Stem Cell Precursors, Transit-Amplifying Progenitors, and their Niche in Developing Hair Follicles. Cell Rep. 2016;14:3001–3018.
[61] Mondal BC, Mukherjee T, Mandal L, et al. Interaction between differentiating cell- and niche-derived signals in hematopoietic progenitor maintenance. Cell. 2011;147(7):1589–1600.
[62] Herrera SC, Bach EA. JNK signaling triggers spermatogonial dedifferentiation during chronic stress to maintain the germline stem cell pool in the Drosophila testis. eLife. 2018;7:e36095.
[63] Brawley C, Matunis E. Regeneration of male germline stem cells by spermatogonial dedifferentiation in vivo. Science. 2004;304(5675):1331–1334.